alternation is good evidence that conjugation extends beyond the first phosphorus atom and is explicable in terms of conjugation of the fluorophenyl group with the homomorphic π system in the phosphonitrile, transfer of charge from the para position being greatest to fluorophosphonitrilic rings containing $4m + 2$ π electrons, *i.e.*, the N_3P_3 and N_5P_5 rings.[37] The different behavior of the monofluorophenyl derivatives may be a result of different steric requirements, and further work is needed to find out. In both series, the ring size variation is small, suggesting that the strong conjugation indicated by the mean chemical shifts relays negative charge principally to the phenyl-substituted phosphorus atom.

(37) Delocalization effects are attenuated rapidly with increase of ring size on account of the different electronegativities of phosphorus and nitrogen.

Acknowledgment.—We thank Mr. R. Burton for the nmr spectra, Mr. P. Borda for the microanalyses, Mr. E. Bichler for help with the preparation of the phosphonitrilic fluorides, and the National Research Council of Canada for financial support.

CONTRIBUTION FROM THE DEPARTMENT OF CHEMISTRY, THE FLORIDA STATE UNIVERSITY, TALLAHASSEE, FLORIDA 32306

Variable-Temperature Proton Nuclear Magnetic Resonance Spectra of Borazine and Borazine-^{10}B

BY EDWARD K. MELLON,* BEATRICE M. COKER, AND PATRICK B. DILLON[1]

Received October 14, 1971

Variable-temperature proton nmr spectra of borazine and borazine-^{10}B are analyzed for chemical shifts, coupling constants, and line widths. The line width data suggest that the broadening is due to a combination of quadrupolar relaxation resulting from the high-spin nuclei present and long-range spin coupling. Three models, including one involving computer simulation of spectra with large constant intrinsic line widths, are tested for applicability for estimating the spin–lattice relaxation times T_{1B} and T_{1N} using Arrhenius plots. The preferred model yields estimates of 1.95 kcal/mol for the average activation energy for molecular reorientation of borazine and 3.6 and 1.5 MHz for the effective quadrupole coupling constants of ^{11}B and ^{14}N, respectively.

Introduction

The proton nmr spectrum of borazine, **1**, consists of broad lines,[2,3] whose number is determined by spin–spin coupling between pairs of nuclei consisting of one proton and one high-spin nucleus, the high-spin

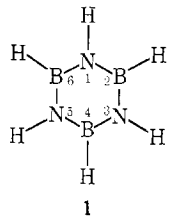

1

nuclei present in appreciable abundance being ^{10}B ($I = 3$, 18.8%), ^{11}B ($I = {}^3/_2$, 81.2%), and ^{14}N ($I = 1$, 99.6%). Line broadening in the proton nmr spectrum of borazine results in part from a relaxation effect involving the nuclear quadrupole moments of the high-spin nuclei. In favorable cases such broadening can be analyzed to yield estimates of nuclear quadrupole coupling constants and activation energies for molecular reorientation.

Pople[4] has presented a theoretical treatment of the quadrupolar relaxation of protons spin coupled to ^{14}N nuclei and subsequent theoretical work has dealt with protons coupled to nuclei with $I = {}^3/_2$ through ${}^7/_2$, and $I = {}^9/_2$.[5] The quadrupolar relaxation model has been used in a discussion of the proton nmr spectra of lithium borohydride, trimethylamine–borane-^{10}B, and *N*-tri(methyl-d_3)borazine-^{10}B[6] and in the analysis of the ^{19}F nmr spectra of BF_3 and ClO_3F.[5] The variable-temperature ^{19}F nmr spectra of NbF_6^- indicate that quadrupolar relaxation is the dominant mechanism at low temperatures while chemical exchange predominates at temperatures above 87°.[5]

In this paper the temperature dependences of the proton nmr spectra of borazine and of borazine-^{10}B are analyzed in terms of quadrupole broadening and of intrinsic line widths arising from long-range spin coupling. In addition, computer-simulated spectra involving quadrupolar broadening in the presence of appreciable constant intrinsic line widths for $I = 1$ and $I = {}^3/_2$ are presented.

Experimental Section

Borazine of normal isotopic content was prepared by the sodium borohydride reduction of tri-*B*-chloroborazine.[7] The product was suitable for chemical shift and coupling constant determinations and for dilution studies but contained impurities which could not be removed by repeated trap-to-trap distillation and which exhibited absorptions near the two high-field components of the ^{11}B quartet. Consequently, the borazine sample (containing 2

(1) Undergraduate research participant.

(2) E. K. Mellon, Jr., and J. J. Lagowski, *Advan. Inorg. Chem. Radiochem.*, **5**, 259 (1963).

(3) K. Ito, H. Watanabe, and M. Kubo, *J. Chem. Phys.*, **32**, 947 (1960).

(4) J. A. Pople, *Mol. Phys.*, **1**, 168 (1958).

(5) M. Suzuki and R. Kubo, *ibid.*, **7**, 201 (1964); J. Bacon, R. J. Gillespie, and J. W. Quail, *Can. J. Chem.*, **41**, 3063 (1963); J. Bacon, R. J. Gillespie, J. S. Hartman, and U. R. K. Rao, *Mol. Phys.*, **18**, 561 (1970); D. W. Aksnes, S. M. Hutchinson, and K. J. Packer, *ibid.*, **14**, 301 (1968); G. M. Whitesides and H. L. Mitchell, *J. Amer. Chem. Soc.*, **91**, 2245 (1969).

(6) H. Watanabe, T. Totani, M. Ohtsuru, and M. Kubo, *Mol. Phys.*, **14**, 367 (1968).

(7) L. F. Hohnstedt and D. T. Haworth, *J. Amer. Chem. Soc.*, **82**, 89 (1960).

mol % TMS) for line shape measurements was prepared by pyrolysis of the solid adduct formed from diborane and ammonia at 25°.[8] Borazine-^{10}B (doped with *ca.* 4 mol % TMS) was prepared similarly from ammonia and diborane-^{10}B, which in turn was obtained from $CaF_2 \cdot {}^{10}BF_3$ (Oak Ridge National Laboratory) containing 95.96% ^{10}B.[9] Isotopic purities of the diborane-^{10}B and of the borazine-^{10}B were monitored by mass spectroscopy.[10] The borazine and borazine-^{10}B samples prepared by pyrolysis also contained traces of impurities which, however, did not interfere with line shape measurements. All compounds were manipulated using conventional high-vacuum preparative techniques; samples for nmr measurements were sealed under vacuum into 5-mm Pyrex nmr tubes.

Variable-temperature nmr spectra at 60 MHz were recorded with a Varian A-60 analytical spectrometer equipped with a V-6040 nmr variable-temperature controller. The sample temperature (accurate to ±1°) was calculated from observed chemical shifts of external methanol samples (for temperatures below 40°) and from ethylene glycol chemical shifts (for temperatures above 40°).[11] Chemical shift and coupling constant frequencies were calibrated by side bands generated with a Hewlett-Packard 200-CDR audio oscillator, and frequency separations between the side bands and the TMS resonance were measured with a Hewlett-Packard 523-DR electronic counter.

The 90-MHz spectra were recorded with a Bruker HFX-90 spectrometer, equipped with a Brucker B-ST 100/700 temperature controller, and temperature settings were corrected with methanol and ethylene glycol. A complication in the temperature correction resulted from the lack of an internal lock standard (a requirement for operation of the Bruker spectrometer used) in the temperature standards supplied by Varian, which made it necessary to lock on the upfield signal in the spectrum of each sample and measure the chemical shift of the downfield absorption. Chemical shifts were then transformed to values appropriate to 60 MHz and temperatures were calculated.[11] Since the spectrum of methanol at temperatures below 270°K has a multiplet structure, a graphical procedure was developed to determine onto which component of the upfield doublet the spectrometer was locked.

Simulated spectra were calculated as illustrated by Abragam[12] except that the following intrinsic line widths were inserted: ^{14}N–H, 14.0 Hz; ^{11}B–H, 27.7 Hz. Calculations were performed on an IBM 360-75 computer at the University of California at Santa Barbara *via* a remote terminal connection. On-line system language was used and the simulated spectra were plotted on a Houston Omnigraphic digital plotter connected to the remote terminal.

Results and Discussion

Chemical Shifts and Coupling Constants.—Borazine chemical shifts and coupling constants are concentration independent within the limits of accuracy possible in dilute solutions in CCl_4. The ^{11}B–H chemical shift is δ −4.46 ± 0.02 ppm in the temperature range −40 to +80°. The ^{14}N–H chemical shift exhibits a slight temperature variation from δ −5.47 at −40° to δ −5.40 at 60° with a 25° value of δ −5.42 ± 0.03 ppm. The ^{11}B–H and ^{14}N–H coupling constants are constant above −20°; below this temperature spectral collapse causes apparent shifts. In the range −20 to +80° the coupling constants are $J_{^{11}B-H}$ = 138.4 ± 0.5 Hz and $J_{^{14}N-H}$ = 55.1 ± 0.2 Hz.

Quadrupolar Relaxation.—Nmr signals from nuclei with quadrupole moments are generally broad because coupling of the quadrupole moment with fluctuating field gradients in the molecular environment provides the dominant route for spin–lattice relaxation of the nuclear spins in the magnetic field. In this case,[13-15] the average spin–lattice relaxation time for the high-spin nucleus (nucleus "X") is

$$\frac{1}{T_{1X}} = \left(\frac{3}{40}\right)\left(\frac{2I+3}{I^2(2I-1)}\right)\left(1+\frac{\eta^2}{3}\right)\left(\frac{e^2qQ}{h}\right)^2\tau_c \quad (1)$$

where the relaxation times for each of the spin states of nucleus X are proportional to T_{1X}. Here, τ_c is the correlation time for molecular reorientation, eQ is the nuclear quadrupole moment, η and eq are the components of the field gradient tensor, I is the nuclear spin, and T_{1X} is the spin–lattice relaxation time for nucleus X.

If a spin $^1/_2$ nucleus (nucleus "A") is spin coupled to the high-spin nucleus, the multiplet components of the half-spin nuclear resonance are also broadened, and spin coupling is eventually completely averaged at the limit of very fast interchange of spin states by nucleus X. This process for a hydrogen nucleus coupled to a high-spin nucleus in one of its spin states is described by an effective relaxation time, $(T_{1A})_{eff}$

$$T_{2A} = (T_{1A})_{eff} \propto T_{1X} \quad (2)$$

Here it is assumed that the spin–spin and spin–lattice relaxation times for nucleus A are equal.[15]

The simplest model for molecular correlation, which presupposes a single correlation time for molecular reorientation, gives rise to the extended Debye relation

$$\tau_c = 4\pi a^3\eta/3kT \quad (3)$$

where a is the radius of the molecule (assumed to be spherical) and η is the viscosity in poise. Thus, according to this model, T_{1X}^{-1} is directly proportional to the viscosity of the nmr sample and inversely proportional to the product of the density and the absolute temperature.

Molecules which contain protons which are spin coupled to high-spin nuclei yield relatively sharp multiplet proton spectra in the limit of high temperature and/or symmetrical electronic environment (*i.e.*, small eq and η) about the high-spin nucleus. Such a case where quadrupolar broadening is essentially absent (due to the tetrahedral symmetry of the boron chemical environment and to the absence of proton exchange) is illustrated by the proton nmr spectrum of $NaBH_4$ in strongly basic aqueous solution (Figure 1) recorded as a part of this study. In contrast, spectra of protons coupled to high-spin nuclei consist of narrow singlets at the limit of low temperature and/or unsymmetrical electronic environment. Intermediate conditions yield spectra consisting of broadened multiplets or singlets.[4,5] The overall features of such proton spectra are functions of the chemical bonding environment of the high-spin nucleus, of the temperature, and, in the case of solutions, of the viscosity of the solvent.[5]

Experimental Spectra.—The 90-MHz proton nmr spectra of borazine (normal isotopic abundance) are shown in the temperature range −40 to +59° in Figure

(8) K. Niedezu and J. W. Dawson, "Boron-Nitrogen Compounds," Springer-Verlag, Berlin, 1965, p 86.

(9) A. C. Graves and D. K. Froman, "Miscellaneous Physical and Chemical Techniques of the Los Alamos Project," McGraw-Hill, New York, N. Y., 1952, p 153.

(10) B. M. Coker, M.S. Thesis, The Florida State University, Tallahassee, Fla., 1970.

(11) A. L. Van Geet, *Anal. Chem.*, **40**, 2227 (1968).

(12) A. Abragam, "Principles of Nuclear Magnetism," Oxford University Press, London, 1961, pp 447–451, 501–506; H. S. Gutowsky, R. L. Vold, and E. J. Wells, *J. Chem. Phys.*, **43**, 4102 (1965).

(13) E. A. C. Lucken, "Nuclear Quadrupole Coupling Constants," Academic Press, London, 1969.

(14) W. B. Moniz and H. S. Gutowsky, *J. Chem. Phys.*, **38**, 1155 (1963).

(15) H. G. Hertz in "Progress in N.M.R. Spectroscopy," Vol. 3, J. W. Emsley, J. Feeney, and L. H. Sutcliffe, Ed., Pergamon Press, Oxford, 1967, pp 159–230.

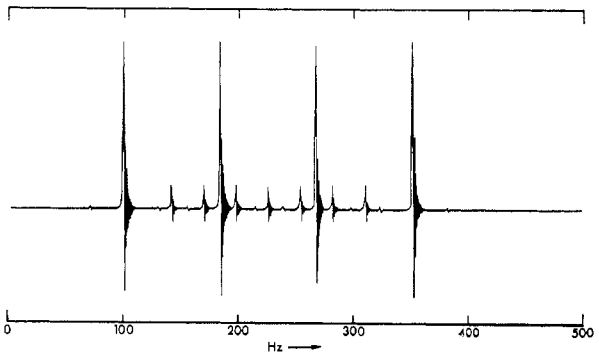

Figure 1.—Proton nmr spectrum (60 MHz) of a saturated solution of $NaBH_4$ in 1.8 *M* aqueous NaOH.

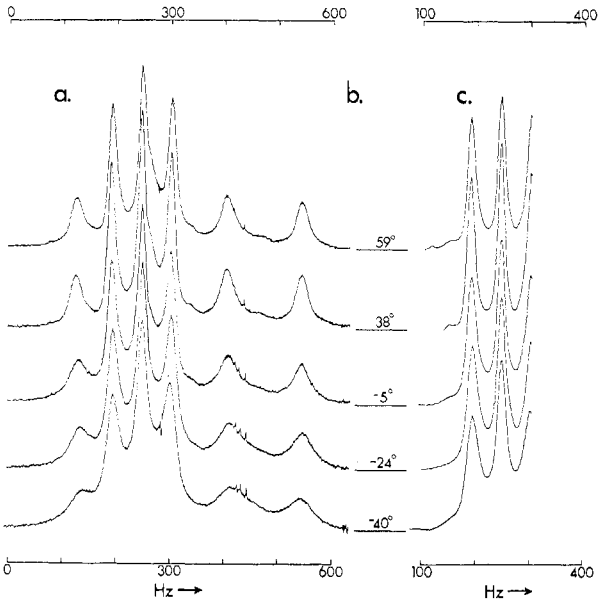

Figure 2.—(a) Variable-temperature (90 MHz) proton nmr spectra of borazine. From the left the broad absorptions are designated B-1, N-1, N-2, N-3, B-3, and B-4 (see text). Absorption B-2 is obscured by the N–H triplet. (b) Temperatures at which the spectra were determined. The horizontal line beneath each temperature is the base line for the spectrum determined at that temperature (series a) and for the ^{14}N–H subtracted spectrum (series c). (c) The ^{14}N–H spectra obtained by subtracting the ^{11}B–H and ^{10}B–H spectra from the experimental spectra (series a).

2 and those of borazine-^{10}B in the range −42 to +85° in Figure 3. There is no significant difference in line widths between spectra recorded at 90 MHz and at 60 MHz. The borazine spectra are broadened to such an extent that rather high recorder gain settings were used in recording the spectra; however, radiofrequency power levels were carefully adjusted to preclude saturation. One consequence of the spectral recording conditions used is that trace impurities became evident in the spectra—note the absorptions at *ca.* 420 Hz in Figure 2 and in the spectrum reported by Kubo, *et al.*[3] These impurities are, however, present at concentrations too small to alter the present analysis. The presence of the TMS lock absorption to the immediate right of the spectra made phase adjustment quite difficult. As a result, the spectra were recorded and analyzed an average of four times before acceptably phased spectra were obtained. Our acceptability criterion for phasing was that the ^{14}N–H spectrum

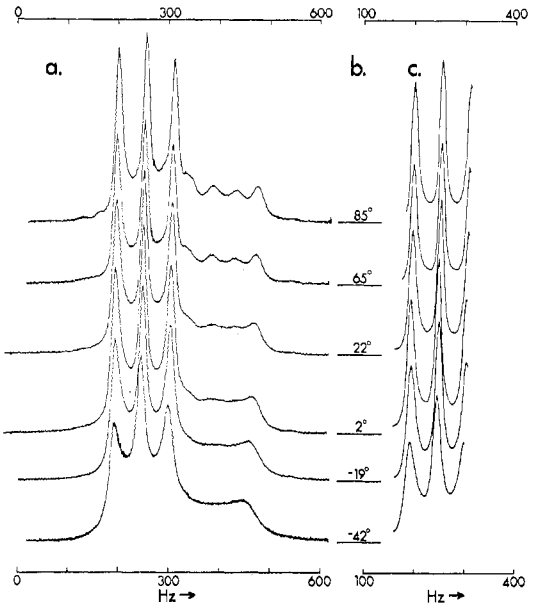

Figure 3.—(a) Variable-temperature (90 MHz) proton nmr spectra of borazine-^{10}B. The three most intense broad absorptions are designated (from the left) N-1, N-2, and N-3. (b) Temperatures and base lines (see Figure 2). (c) Subtracted ^{14}N–H spectra.

(Figures 2c and 3c) remaining after the ^{11}B–H and ^{10}B–H spectra had been subtracted be in phase.

Line widths obtained from the spectra are shown in Figure 4. If the components of the proton multi-

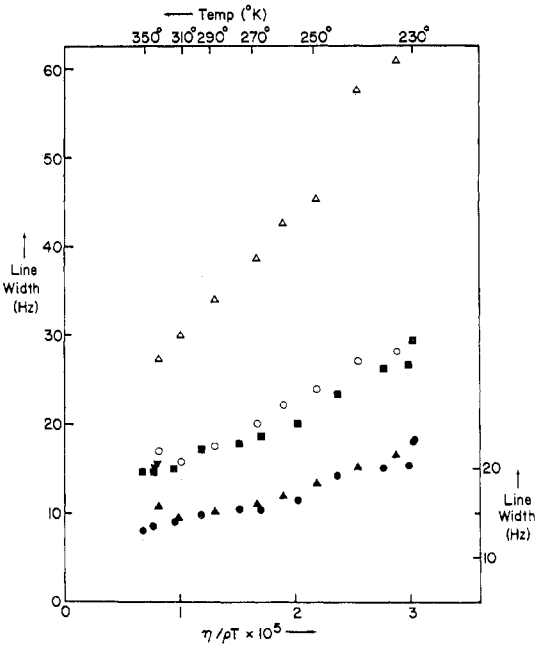

Figure 4.—Line widths of the ^{11}B–H and ^{14}N–H lines from the proton nmr spectra of borazine and borazine-^{10}B. Data symbols: N-2 (90-MHz borazine-^{10}B, right-hand ordinate), ●; N-2 (90-MHz borazine, right-hand ordinate), ▲; N-1 (90-MHz borazine-^{10}B, left-hand ordinate), ■; N-1 (90-MHz borazine, left-hand ordinate), ○; N-1 (60-MHz borazine-^{10}B, left-hand ordinate), ▼; B-4 (90-MHz borazine, left-hand ordinate), △.

plets are designated as B-1, B-2, B-3, and B-4 (^{11}B–H quartet reading from low frequency) and N-1, N-2, and N-3 (^{14}N–H triplet reading from low frequency), respectively, the data ranges for the line widths over

the temperature ranges studied are as follows: B-4, 27.4–60.8 Hz; N-1, 15.7–29.4 Hz; N-2, 13.0–23.0 Hz. The ^{11}B–H line width at half-height (the "line width" as used in this paper) for B-4 was first estimated approximately from each spectrum (Figure 2a) and used to plot a lorentzian tail for B-3. A corrected peak height for B-4 was thus obtained from which the line width (Figure 4) was finally measured. The ^{14}N–H line widths were estimated as follows: The centers of the B–H and N–H multiplets (Figures 2a and 3a) were located using chemical shift data and the ^{10}B–H and ^{11}B–H multiplets were graphically subtracted to reveal the ^{14}N–H multiplets (Figures 2c and 3c). These were resolved into lorentzian components with a Du Pont 310 curve resolver. The sum spectra of the three lorentzian components were in excellent agreement with the experimental spectra. The line widths were estimated from the lorentzian lines derived from N-1 and N-2; the N-3 line was not used, being too close to the center of the ^{11}B–H and ^{10}B–H multiplets. We found reasonable agreement between the individual lorentzian lines estimated with the curve resolver and lorentzian lines calculated from the measured line widths.

The ^{11}B–H line widths (Figure 4) vary linearly with $\eta/\rho T$[16] throughout the entire data range examined while the ^{14}N–H line widths vary linearly with $\eta/\rho T$ only above $\eta/\rho T = 1.4 \times 10^{-5}$. This indicates that the broadening is quadrupolar in nature, although eq 1 and 3 do not predict an intercept. The ^{11}B–H line widths are described by a straight-line slope $m = 1.64 \times 10^6$ cm^2/sec deg and intercept $b = 12.7$ Hz with an average deviation of ±1.6 Hz in the line widths. Straight lines which describe the ^{14}N–H data at $\eta/\rho T$ values greater than 1.4×10^{-5} have the following parameters: N-1 (90-MHz borazine): $m = 6.84 \times 10^5$ cm^2/sec deg, $b = 9.00$ Hz, average deviation ±0.34 Hz, N-2 (90-MHz borazine): $m = 4.635 \times 10^5$, $b = 8.202$, average deviation ±0.06; N-1 (90-MHz borazine-^{10}B): $m = 7.08 \times 10^5$, $b = 6.57$, average deviation ±0.60; N-2 (90-MHz borazine-^{10}B): $m = 4.42 \times 10^5$, $b = 8.25$, average deviation ±0.66. It appears that in the borazine spectra the N-1 absorption is 1.5–2.0 Hz broader and the N-2 absorption is 0.3–0.5 Hz broader than in the borazine-^{10}B spectra.

Computer-Simulated Spectra.—We first calculated a set of ^{14}N–H spectra with a variety of values of T_{1N} following the Pople–Abragam method exactly.[5,12] This method assumes the multiplet components to be infinitely sharp in the absence of quadrupolar broadening; thus, the ^{14}N–H triplet in the limit of very long T_{1N} consists of three lines with peak heights in the ratio 2:3:2. This is not realistic physically, since in the limit of very long T_{1X}, other relaxation mechanisms become dominant and all multiplet components in spectra of this type become equal in height (Figure 1). Only at the lowest temperatures did our experimental ^{14}N–H multiplets approach 2:3:2 height ratios (Figures 2c and 3c), being much closer to 1:1:1 at the highest temperatures where measurements were possible.

The experimental spectra were of some aid in choosing a magnitude for the intrinsic line width for the ^{14}N–H lines. That the experimental ^{14}N–H line widths (Figure 4) tend toward the horizontal at $\eta/\rho T$ values less than 1.4×10^{-5} suggested to us that these lines might have appreciable intrinsic line widths due to two-bond spin coupling between the ^{14}N–H hydrogen and the two nearest boron nuclei and, possibly, to longer range spin coupling. The ^{14}N–H multiplet components are slightly broader in borazine than in borazine-^{10}B which is evidence that coupling to boron is a major contributor to the intrinsic line width.[17] The experimental ^{14}N–H multiplets do not exhibit fine structure resulting from coupling between the ^{14}N–H proton and the two nearest boron nuclei (Figures 2c and 3c); however, this is probably due to a combination of the small magnitude of the

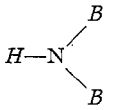

coupling constant, the number of lines in the multiplet, and quadrupolar relaxation. Broad featureless absorptions of this sort are common among the nmr spectra of bridging protons in boron hydrides.[18]

A series of spectra was generated using a *constant* intrinsic line width (Abragam's $1/\tau^5$) equal to 14.0 Hz, and a sample spectrum from this run is illustrated in Figure 5. Rather than reproduce a series of such spectra, we have plotted several parameters from the simulated spectra *vs.* log $(1/T_{1N})$ in Figure 6. These are derived from a, the uncorrected trough height, c, the uncorrected peak height of N-1, d, the uncorrected peak height of N-2, e, the true line width of N-1, and f, the true line width of N-2. Parameter b (not plotted) is the true half-height of N-1. The parameters plotted (which are independent of the intensity of the spectra) are a/c, a/d, c/d, e, f, and J_{NH}, the apparent

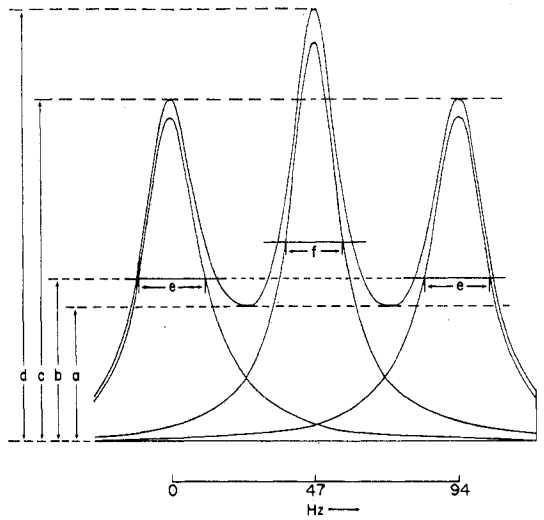

Figure 5.—Computer-simulated ^{14}N–H triplet with intrinsic line width 14.0 Hz where $T_{1N} = 0.1089$ sec. The multiplet is resolved into lorentzian lines of width e (N-1 and N-3) and f (N-2), respectively. Parameter b is the half-height of the N-1 and N-2 lorentzian components, a is the trough height of the unresolved multiplet, and c and d are the peak heights of N-1 and N-2, respectively, in the unresolved multiplet.

(16) Viscosity and density data were obtained from L. P. Eddy, S. H. Smith, and R. R. Miller, *J. Amer. Chem. Soc.*, **77**, 2105 (1955).

(17) J. W. Akitt, *J. Magn. Resonance*, **3**, 411 (1970).

(18) G. R. Eaton and W. N. Lipscomb, "NMR Studies of Boron Hydrides and Related Compounds," W. A. Benjamin, New York, N. Y., 1969.

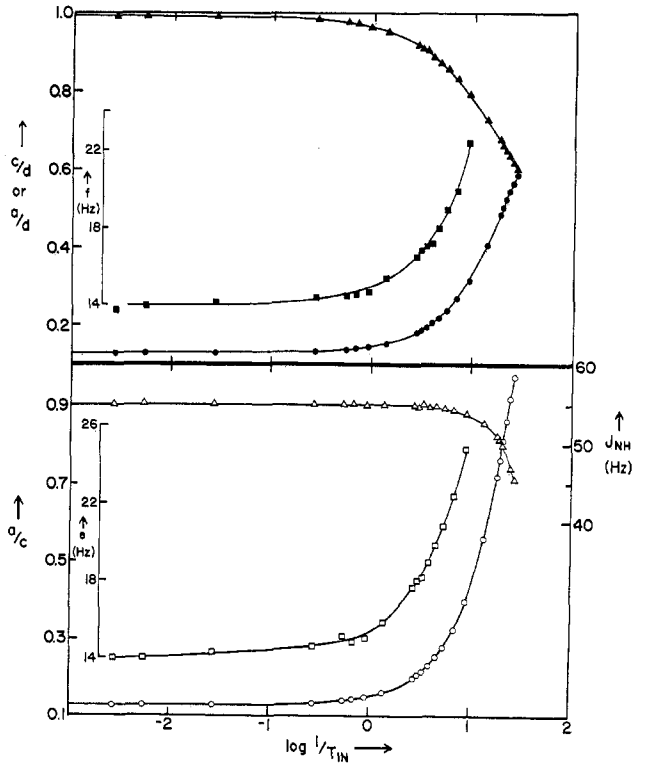

Figure 6.—Description of a series of computer-simulated ^{14}N–H triplets with intrinsic line width 14.0 Hz. See Figure 5 for definitions of *a*, *c*, *d*, *e*, and *f*. Data symbols: *a*/*c*, ○ (lower left-hand ordinate); *e*, □ (lower center ordinate); apparent coupling constant J_{NH}, △ (right-hand ordinate); *a*/*d*, ● (upper left-hand ordinate); *f*, ■ (upper center ordinate); *c*/*d*, ▲ (upper left-hand ordinate).

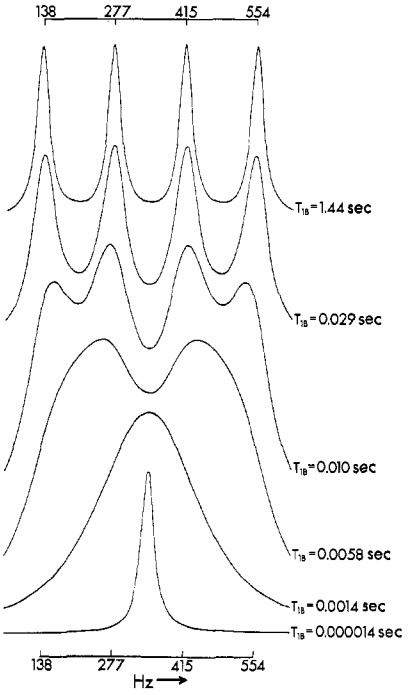

Figure 7.—Representative computer-simulated ^{11}B–H quartets calculated with intrinsic line width 27.7 Hz.

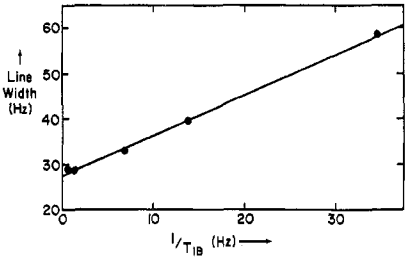

Figure 8.—Line widths of Lorentzian components of the computer-simulated ^{11}B–H quartet (T_{1B} > 0.029 sec) *vs.* $1/T_{1B}$.

coupling constant. The apparent coupling constant is somewhat less in the spectrum in Figure 5 than 55.1 Hz (the limiting value of $J_{^{14}N-H}$) because this spectrum corresponds to a T_{1N} value where collapse is well advanced. The simulated spectra were resolved to yield lorentzian multiplet components and true line widths in the same way as the experimental spectra; plots of the true line widths of the resolved peaks N-1 and N-2 *vs.* $1/T_{1N}$ yielded straight lines. Collapse of the simulated spectra is advanced to the point where the last vestige of triplet structure occurs at T_{1N} = 0.0218 sec; representative line widths for the singlet absorption at shorter relaxation times are as follows: T_{1N} = 0.0018 sec, line width 21.3 Hz; T_{1N} = 0.00036 sec, line width 15.6 Hz; T_{1N} = 0.000036 sec, line width 14.6 Hz.

A series of ^{11}B–H quartets with intrinsic line width 27.7 Hz was also generated and representative spectra are plotted in Figure 7. The simulated spectra were resolved into lorentzian components in the same manner as with the ^{14}N–H triplets; Figure 8 represents a plot of the line widths of the lorentzian components *vs.* $1/T_{1B}$.

Relaxation Time Estimates.—The relaxation times T_{1B} and T_{1N} were established by three different models. Model 1 which is suitable when the spectrum is in the region of initial broadening and when the intrinsic line width is at the limit of very small values[4] involves multiplication of the line widths (lw) by an appropriate constant: for N-1, $T_{1N}^{-1} = 5\pi(\text{lw})/3$; for N-2, $T_{1N}^{-1} = 5\pi(\text{lw})/2$; for B-4, $T_{1B}^{-1} = \pi(\text{lw})$. Data estimated in this way make up the top three plots in Figure 9. Model 2 involves the comparison of the experimental spectra with the computer simulated spectra. T_{1B} was estimated by matching the line widths of component B-4 (Figure 4) with those plotted in Figure 8. This procedure was adequate for the estimation of T_{1B} since all spectra were in the region of initial broadening. For the estimation of T_{1N} for each experimental spectrum (Figures 2c and 3c) we used at least five of the six empirical parameters plotted in Figure 6, because the collapse of the ^{14}N–H triplets is more pronounced in the temperature range studied. The T_{1N} values so obtained were then averaged to give the bottom plot shown in Figure 9.

In model 1 the intrinsic line widths are completely ignored; in model 2 a slight overestimate of the high-temperature intrinsic width of T_{1N} and a more generous overestimate for T_{1B} are indicated by the negative intercepts of the plots. Also in model 2 the T_{1X} values are calculated with the assumption of *constant* intrinsic line width. Now, the data in Figure 4 indicate that the intrinsic line width is either constant or varies in a linear manner with $\eta/\rho T$; in this latter case T_{1X} values estimated with model 2 should become increasingly unreliable as $\eta/\rho T$ becomes larger.

Model 3 involves estimating the T_{1X} values from the

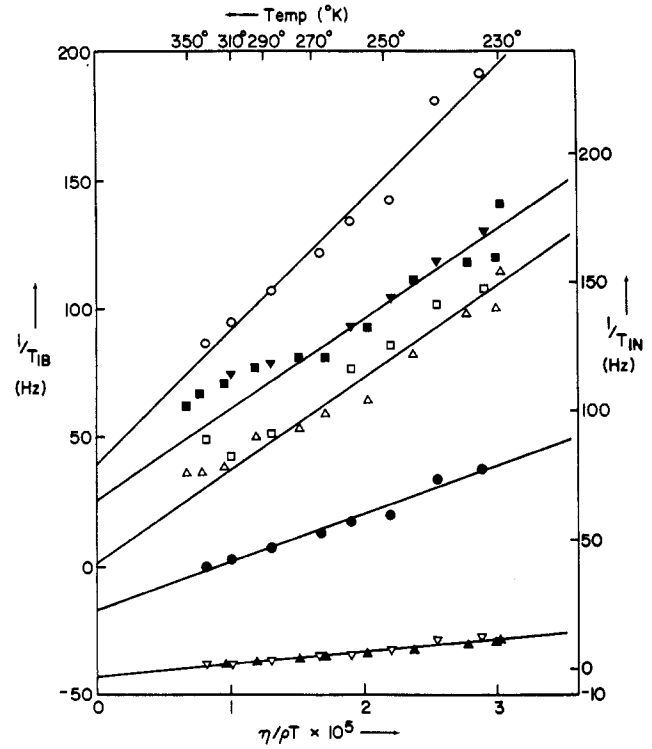

Figure 9.—Estimated relaxation times *vs.* $\eta/\rho T$. Data symbols: T_{1N} (borazine) estimated by matching experimental ^{14}N–H spectra (Figure 2c) with the empirical parameters in Figure 6, ▽ (right-hand ordinate); T_{1N} (borazine-^{10}B) obtained in the same way, ▲ (right-hand ordinate); T_{1B} (borazine) estimated by matching B-4 line widths with those plotted in Figure 8, ● (left-hand ordinate); T_{1N} (borazine) estimated from N-1 line widths by $T^{-1}{}_{1N} = 5\pi(\text{lw})/3$, □ (right-hand ordinate); T_{1N} (borazine-^{10}B obtained in the same way, △ (right-hand ordinate); T_{1N} (borazine) estimated from N-2 line widths by $T^{-1}{}_{1N} = 5\pi(\text{lw})/2$, ▼ (right-hand ordinate); T_{1N} (borazine-^{10}B) obtained in the same way, ■ (right-hand ordinate); T_{1B} (borazine) estimated from B-4 line widths by $T^{-1}{}_{1B} = \pi(\text{lw})$, ○ (left-hand ordinate).

lines: $T_{1B}{}^{-1} = (5.144 \times 10^6\ \text{cm}^2/\text{sec deg})(\eta/\rho T)$ and $T_{1N}{}^{-1} = (3.532 \times 10^6\ \text{cm}^2/\text{sec deg})(\eta/\rho T)$, which are parallel to those of model 1 and have zero intercepts. Thus model 3 corrects for the temperature-invariant portion of the intrinsic line width while ignoring the temperature-variable portion.

The applicability of these three models was tested by considering the activation energies and intercepts obtained from plots of log T_{1X} *vs.* $1/T$°K. In general, these activation parameters are loosely connected[19] with the process of molecular reorientation in the liquid state; thus the ^{14}N and ^{11}B data should yield identical parameters. The activation energies and intercepts were as follows: for model 1: 1.24 kcal/mol and −1.10 (T_{1B}), 1.27 kcal/mol and −0.97 (T_{1N}, N-1), 1.04 kcal/mol and −1.25 (T_{1N}, N-2); for model 2: 4.61 kcal/mol and 2.70 (T_{1B}), 2.83 kcal/mol and 1.61 (T_{1N}); for model 3: 1.95 kcal/mol and −0.34 (T_{1B}), 1.95 kcal/mol and −0.18 (T_{1N}). The disagreement of the ^{14}N and ^{11}B parameters from model 2 indicates that the intrinsic line width is not independent of temperature. This renders model 2 the least attractive. Model 3 is then preferred to model 1 because the temperature-invariant portion of the intrinsic line width is considered explicitly. Such a comparison of parameters estimated with T_{1B} and T_{1N} is valid only if the principal axes of the field gradient coordinate systems of the ^{14}N and ^{11}B molecular environments are parallel. Although the activation energy for molecular reorientation for a hexagonal planar molecule such as borazine is probably an average of more than one energy reflecting the presence of molecular rotational anisotropy, it is of interest to note that a similar treatment of perdeuteriobenzene yielded an activation energy of 1.86 kcal/mol[20] (compare model 3).

Rough estimates of the effective quadrupole coupling constants $|(1 + \eta^2/3)^{1/2}(e^2qQ/h)|$ of ^{14}N and ^{11}B in borazine can be made from the slopes of the lines presented as model 3 and eq 1 and 3: the values are 3.6 MHz (^{11}B) and 1.5 MHz (^{14}N), respectively. Such estimates from nmr line widths do not yield the signs of the coupling constants nor separate values for η and eq, nor do they give the orientation of the field gradient coordinate system with respect to the molecular framework. These values, however, are useful in the initial search for pure quadrupole reonance lines, and, more significantly, information about bonding may be obtained by a comparison of data for closely similar molecules.[18] The ^{14}N coupling constant derived here probably contains a substantial contribution from the asymmetry parameter; a pure nuclear quadrupole resonance study of pyrrole[18] yielded e^2qQ/h = 2.06 MHz and η = 0.269. However, asymmetry parameters in trigonal boron atoms lacking axial symmetry are generally believed to be small;[21,22] thus, approximating η as zero in borazine and assuming the z axis of the field gradient coordinate system to be perpendicular to the plane of the borazine ring, we estimate e^2qQ/h for ^{11}B to be 3.6 MHz. In valence bond formalism this leads to an estimate of 67% double-bond character in borazine as compared with 47% estimated earlier.[21] An examination of the proton nmr spectrum of *N*-tri(methyl-d_3)borazine-^{10}B[6] indicates that the analysis presented here could profitably be extended to other borazine systems.

It should be possible experimentally to test the T_{1N} values estimated from model 3 by measuring the temperature variation of the ^{15}N–H proton absorptions in borazine-^{15}N. The results of such a study would have significant implications as a model system for the boron hydrides and carboranes where extensive long-range spin coupling to quadrupolar nuclei, as well as local quadrupolar relaxation, may be expected.

Acknowledgment.—Acknowledgment is made to the donors of The Petroleum Research Fund, administered by the American Chemical Society, for support of this research. The authors also wish to express their appreciation to M. Goldman, R. R. Rosanske, and B. B. Garrett for several valuable conversations.

(19) J. G. Powles and M. C. Gough, *Mol. Phys.*, **16**, 349 (1969).

(20) D. E. Woessner, *J. Chem. Phys.*, **40**, 2341 (1964).

(21) M. A. Ring and W. S. Koski, *ibid.*, **35**, 381 (1961), and references contained therein.

(22) K. Wiedemann and J. Voitlaender, *Z. Naturforsch. A*, **24**, 566 (1969).